Population expansion, isolation and selection: novel insights on the evolution of color diversity in the strawberry poison frog

Marcelo Gehara, Kyle Summers & Jason L. Brown

Evolutionary Ecology

ISSN 0269-7653
Volume 27
Number 4

Evol Ecol (2013) 27:797-824
DOI 10.1007/s10682-013-9652-0

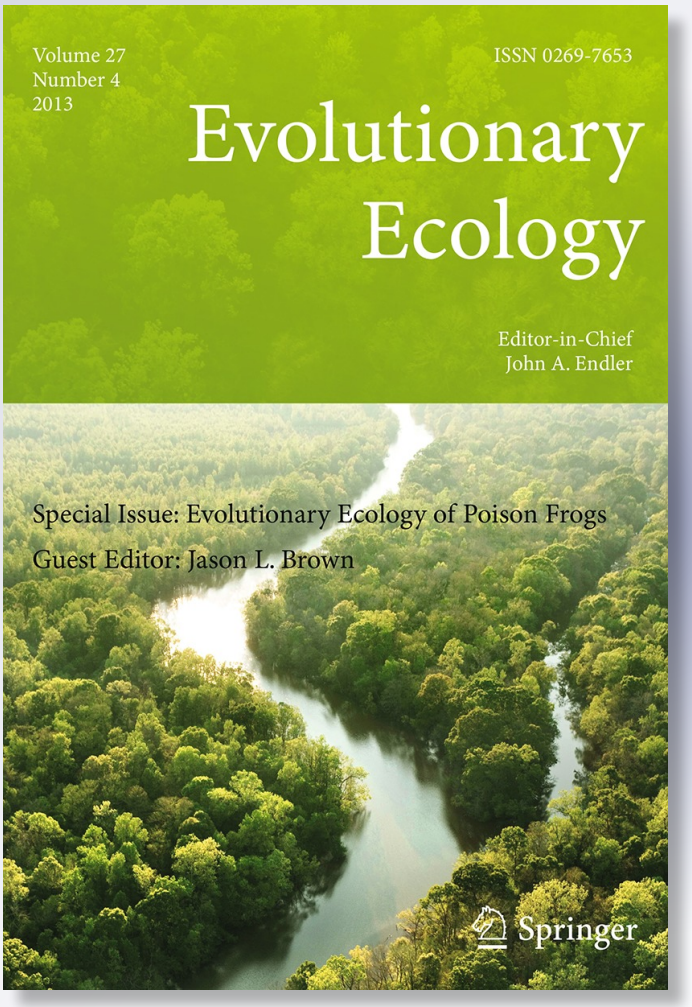

Springer

Evol Ecol (2013) 27:797–824
DOI 10.1007/s10682-013-9652-0

ORIGINAL PAPER

Population expansion, isolation and selection: novel insights on the evolution of color diversity in the strawberry poison frog

Marcelo Gehara · Kyle Summers · Jason L. Brown

Received: 29 September 2012 / Accepted: 6 May 2013

Abstract The evolutionary mechanisms causing intraspecific diversity in aposematic color and pattern remain enigmatic. The strawberry poison frog (*Oophaga pumilio*) has diversified into a broad array of colors that span the visible spectrum. The most divergent phenotypes of *O. pumilio* are restricted to separate islands in the Bocas del Toro archipelago in western Panama, whereas throughout the majority of its range (from Nicaragua to western Panama) this species exhibits a single red phenotype. During the Holocene, sea-levels increased and changes in climate caused shifts in habitat through time. In the Bocas del Toro archipelago, rising sea-levels isolated previously connected populations in higher elevation habitats (forming islands). In this study we use historic measures of demography, ancestral distribution estimates, spatiotemporally explicit demographic models and genetic simulations to investigate the genetic consequences of the isolation due to sea-level changes and demographic processes mediated by recent climatic fluctuations. We then evaluate the role of these factors in the evolution of color in *O. pumilio* by measuring and comparing the deep coalescence of a neutrally evolving nuclear gene and a hypothetical autosomal coloration gene. Our results support a major role for recent population expansion and reduced gene flow (from isolation on islands) in the diversification of color across populations.

Keywords Dendrobatidae · Demography · Color evolution · Dynamic histories · Natural selection · Sexual selection

M. Gehara
Department of Evolutionary Biology, Zoological Institute, Technical University of Braunschweig, Braunschweig, Germany

K. Summers
Department of Biology, East Carolina University, Howell Science Complex, Greenville, NC 27858, USA

J. L. Brown (✉)
Department of Biology, Duke University, 125 Science Dr., Durham, NC 27705, USA
e-mail: jason.l.brown@duke.edu

Introduction

For many aposematic species their color and pattern is largely conserved throughout their range. In some cases, several aposematic species converge (or adverge) on a single phenotype to share benefits from mutual predator deterrence (Müller 1879; Symula et al. 2001). It is thought that a single warning display not only enhances discrimination in educated predators, but also improves learning and memory retention with respect to the toxicity of defended animals (Wallace 1867; Darwin 1887; Poulton 1890).

The evolutionary mechanisms causing intraspecific diversity in aposematic color and pattern remain enigmatic. In aposematic poison frogs (family Dendrobatidae) dramatic intra-specific phenotypic variation among populations is common (e.g., in *Ranitomeya imitator*, *R. sirensis*, *Dendrobates tinctorius*, *Oophaga histrionica*). One species that may provide insight into the factors driving intraspecific diversity in aposematic signals is *Oophaga pumilio* (formerly *Dendrobates pumilio*, see Grant et al. 2006; Brown et al. 2011), a species that possesses extraordinary phenotypic variation (Fig. 1, Daly and Myers 1967). Throughout a large portion of the range of this species, from Nicaragua to western Panama, most populations possess a bright red dorsum flecked with small black spots and black to blue limbs. In the Bocas del Toro Archipelago, *O. pumilio* exhibits a wide array of phenotypes from green, orange to blue, with different colored (or matching) limbs and varying levels of dark dorsal patterning (Daly and Myers 1967; Summers et al. 2003, 2004). Despite possessing considerable phenotypic variation, populations are monomorphic, with the exception of Isla Bastimentos, a large island with two main color morphs likely controlled by a single Mendelian locus (Richards-Zawacki et al. 2012).

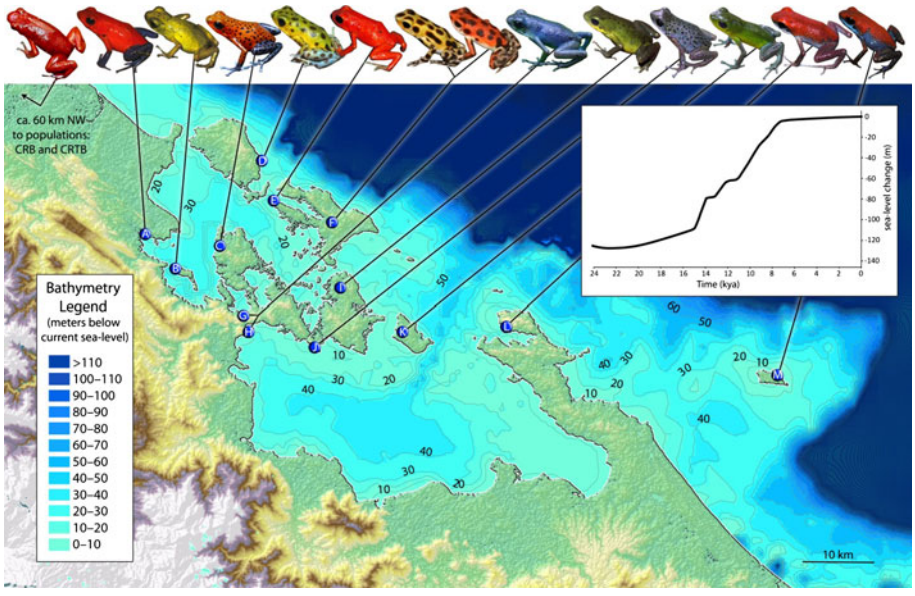

Fig. 1 Focal populations of *O. pumilio*, bathymetry of Bocas del Toro archipelago (data from: GEBCO 2012) and sea-level change since last glacial maximum (Simplified from Fleming et al. 1998; Milne et al. 2005). *Photos* T. Ostrowski. Population name: *A* Almirante, *B* Pastores, *C* San Cristobal, *D* Colón, *E* Solarte, *F* Bastimentos, *G* Tierra, *H* Cauchero, *I* Popa, *J* Loma Partida, *K* Cayo de Agua, *L* Punta Alegre, *M* Escudo de Veraguas

Oophaga pumilio has been the subject of a wide array of studies, focusing on its phylogeography (e.g., Hagemann and Pröhl 2007; Wang and Shaffer 2008; Hauswaldt et al. 2010), sexual selection and female mate choice (e.g., Summers et al. 1999; Reynolds and Fitzpatrick 2007; Maan and Cummings 2009; Richards-Zawacki and Cummings 2011), parental care (e.g., Weygoldt 1980; Brust 1993; Pröhl and Hödl 1999; Summers and Earn 1999), reproductive behavior (e.g., Limerick 1980), life history (e.g., Donnelly 1989; Staudt et al. 2010), territoriality (e.g., Donnelly 1987; Pröhl 1997; Pröhl and Berke 2001, Bee 2003), toxicity (e.g., Daly and Myers 1967; Saporito et al. 2006, 2007) and communication (Bunnell 1973; Meuche et al. 2012). Recent studies have revealed that this species likely comprises a species complex, representing two major mitochondrial linages (Rudh et al. 2007; Hagemann and Pröhl 2007; Wang and Shaffer 2008): a predominantly northern lineage that occurs from Nicaragua to the south-eastern border of Costa Rica and a second predominantly Panamanian lineage centered around the Bocas del Toro Archipelago. These two mitochondrial lineages occasionally admix and some gene flow has been detected among both groups (Hauswaldt et al. 2010). The relationship of the two lineages of *O. pumilio* to other closely related species (*Oophaga vicentei*, *O. speciosa* and *O. arborea*) is currently unresolved and in some studies these species render *O. pumilio* paraphyletic (Hagemann and Pröhl 2007; Hauswaldt et al. 2010; Brown et al. 2010). Despite this convoluted and incompletely understood complex of populations and species, a strong signal of a northern and a southern evolutionary lineage within *O. pumilio* is detectable on the basis of microsatellite markers (Hauswaldt et al. 2010). It therefore appears justified to distinguish two lineages in the present study, *O. pumilio* "N" and *O. pumilio* "S", respectively (Hagemann and Pröhl 2007; Hauswaldt et al. 2010). The main focus here is on the populations from the Bocas del Toro archipelago, which in all analyses have been unequivocally assigned to the Southern *O. pumilio* lineage.

The two lineages of *O. pumilio* demonstrate different phylogeographic patterns that are suggestive of different demographic histories: *O. pumilio* "N" is comprised of divergent populations with relatively deeper mitochondrial (mtDNA) coalescence and higher nucleotide diversity, where haplotypes are separated by more mutations. In contrast, *O. pumilio* "S" comprises a group of closely related individuals with shallower mtDNA coalescence and lower nucleotide diversity, where most mitochondrial haplotypes are separated by a single mutation (Summers et al. 1997; Hagemann and Pröhl 2007; Wang and Shaffer 2008; Hauswaldt et al. 2010; Brown et al. 2010). Some of this divergence could be attributed to normal phylogeographic processes (i.e., isolation-by-distance), especially given that the geographic range of the northern group is an order of magnitude larger than that of the southern group. Consistent with this difference, the Northern lineage exhibits higher levels of genetic and advertisement call diversity. However, in contrast to expectations, little morphological diversity exists in this group (Pröhl et al. 2007).

Mate choice studies on the Bocas del Toro populations of *O. pumilio* "S" demonstrate that most females from monomorphic island populations consistently prefer to court males of their own color/pattern over other males from nearby islands that differ in color/pattern (Summers et al. 1999; Reynolds and Fitzpatrick 2007; Maan and Cummings 2008, 2009; Richards-Zawacki and Cummings 2011). These results suggest that divergent morphs may be reproductively isolated. A recent field study of mate choice on the only polymorphic island population, Isla Bastimentos, demonstrated that only one of the two morphs mated assortatively (Richards-Zawacki et al. 2012).

Summers et al. (1997) initially proposed that sexual selection in combination with geographic isolation and genetic drift could have driven the diversity seen among *O. pumilio* populations in the Bocas del Toro Archipelago. Since then, several hypotheses

have been proposed to explain the rapid evolution of coloration, invoking different roles for selection, drift and demographic processes (Table 1). The following are summaries of the six major hypotheses:

(1) *Dorsal conspicuousness* Maan and Cummings (2009) postulated that female preference for dorsal brightness, not necessarily color, initially drove the divergence in coloration.
(2) *Indicator of toxicity* Maan and Cummings (2012) later demonstrated that color diversity was tightly linked to variation in toxicity, with brighter populations being more toxic. In this hypothesis variation in dorsal coloration is mediated by an interaction between natural selection by predators and sexual selection by female mate choice.
(3) *Geographic isolation*. Due the biogeography of this polytypy, with many divergent phenotypes restricted to separate islands, others have suggested neutral processes played a greater role in the process of color diversification (Wang and Summers 2010; Brown et al. 2010). This hypothesis relies on the combination of restricted gene flow, drift and reduced population sizes due to marine introgression of the Bocas del Toro Archipelago, starting ca. 10kya and not completed until 1kya (Summers et al. 1997; Anderson and Handley 2002; Wang and Shaffer 2008).
(4) *Behavioral isolation* Wang and Summers (2010) used various measures of population structure and gene flow to demonstrate high concordance between dorsal coloration and genetic structure. They concluded that selection (natural or sexual) drove phenotypic divergence resulting in reduced gene flow among divergence phenotypes. Under this hypothesis, divergence is not driven by reduced gene flow caused by geographic barriers among populations, but through selection against immigrant phenotypes.
(5) *Geographic and behavioral isolation* A variant of the latter two hypotheses posits that the underlying mechanism involved the initiation of divergence by genetic drift (with or without founder effects) due to isolation on islands and then the rapid fixation of divergent phenotypes via female mate choice (Summers et al. 1997; Brown et al. 2010).
(6) *Coupled drift* Others have focused solely on divergence via drift in female preference and sexual selection. The hypothesis is considered separate from the Geographic and Behavioral Isolation hypothesis, because this hypothesis does no invoke explicit roles for isolation, population size and other demographic processes (Tazzyman and Iwasa 2010).

The Isthmus of Panama has a dynamic geological and climatic history that likely caused dramatic shifts in habitat through time (Colinvaux 1991; Coates and Obando 1996; Coates et al. 2004). One major driver of these shifts was the pattern of glacial cycles that likely caused many species to track suitable habitat, either up and down the slopes of the Cordilleras (for montane species) or north or south in latitude (Colinvaux et al. 1996; Piperno and Pearsall 1998; Savage 2002). During glacial recessions, sea-levels increased dramatically, isolating previously connected populations in higher elevation habitats (forming islands). For species with limited ecological tolerances, such isolation likely forced populations to adapt to altered local conditions under strong selection.

Instability of climate and habitat over the history of a species has important genetic consequences (Hewitt 1996; Lohse et al. 2011). Distributional shifts can be dramatic and the distributions of ancestral and contemporary populations may be considerably different (e.g., Galbreath et al. 2009; Voje et al. 2009; Graham et al. 2010; Morgan et al. 2011).

Table 1 Major hypothesis and mechanisms concerning the dramatic color divergence of *O. pumilio*

Hypothesis of color divergence	Major mechanism						Summary	Key citation
	Selection		Drift	Demographic				
	Natural (aposematism)	Sexual (female mate choice)	Genetic drift	Geographic isolation	Rapid population expansion	Small population size		
Dorsal conspicuousness		X					Female preference for dorsal brightness, not necessarily color, initially drove the divergence in coloration	Maan and Cummings (2009)
Indicator of toxicity	X	X*					Variation in dorsal coloration is mediated by an interaction between natural selection by predators and sexual selection by female mate choice	*Wang and Shaffer (2008) did not include sexual selection; Rudh et al. (2011); Pröhl and Ostrowski (2011);Maan and Cummings (2012); Hegna et al. (2012)
Behavioral isolation		X					Sexual selection drove phenotypic divergence that resulted in reduced gene flow through selection against immigrant phenotypes	Wang and Summers (2010)
Geographic isolation			X			X	Isolation due to marine introgression. Neutral processes caused divergence.	Wang and Summers (2010); Brown et al. (2010)

Table 1 continued

Hypothesis of color divergence	Major mechanism						Summary	Key citation
	Selection		Drift	Demographic				
	Natural (aposematism)	Sexual (female mate choice)	Genetic drift	Geographic isolation	Rapid population expansion	Small population size		
Geographic and behavioral isolation		X	X	X		X	Isolation due to marine introgression. Drift initiated divergence, then rapid fixation of phenotypes via sexual selection	Summers et al. (1997); Rudh et al. (2007); Brown et al. (2007)
Coupled drift		X	X				Drift in female preference and sexual selection	Tazzyman and Iwasa (2010)
Expansion and isolation		X	X	X*	X		Colonization of Bocas del Toro during Holocene, followed by isolation and dramatic population expansion during late Holocene. Gene surfing initiated divergence then further diverged via sexual selection	This paper. *Geographic isolation is not required, but reduces the strength of selection required

Edmonds et al. (2004) simulated the fate of new mutations arising on the edge of a wave of population expansion. Typically these new mutations would go extinct or remain at low frequencies around their place of origin. However in some cases these new mutations (even deleterious ones) would increase in frequency and be propagated by the wave, reaching very high frequencies and even fixation away from the site of origin. Thus contrary to widespread belief, this suggests that the area with the highest frequency of a mutation is not necessarily the site of origin. Since then, others have demonstrated that mutations can surf on waves (often called gene surfing) more effectively in small populations, and this process is particularly favored in rapidly growing populations with limited dispersal (Klopfstein et al. 2006). In these situations, mutations can often be fixed in newly colonized areas. Thus, many patterns that have been previously attributed to distinct selective processes can actually be explained by demographic processes.

Here we investigate additional factors that may have strongly influenced the divergence in coloration associated with what we term the Expansion and Isolation model. Under this model, *O. pumilio* "S" colonized the Bocas del Toro during the early Holocene when local climate became more suitable. Shortly after colonization, marine introgression isolated populations on islands and during the mid-Holocene the local climate dramatically improved, increasing local population densities. As populations colonized the Bocas del Toro region, the initial divergence (and likely fixation) in coloration resulted from gene surfing (intense genetic drift taking place at the edge of an expanding population). Variations in phenotype were isolated (often among islands), that further diverged via sexual selection, leading to current levels of diversity. We investigated the genetic consequences of the isolation due to sea-level changes and demographic processes mediated by recent climatic fluctuations. We then investigated the potential role of these factors in the evolution of color in *O. pumilio*. Lastly we frame these results in the context of the major hypotheses of color evolution in *O. pumilio*.

Methods

Species distribution models

Species occurrence data for *O. pumilio* (both Northern and Southern lineages) were taken from previous studies (Wang and Shaffer 2008; Brown et al. 2010; Hauswaldt et al. 2010) and represented 38 unique localities ranging from Nicaragua to central Panama. A single species distribution model (SDM) consisting of data from both lineages was generated in Maxent v3.3.3e (Phillips et al. 2006) using the following parameters: random test percentage = 25, regularization multiplier = 1, max number of background points = 10,000, replicates = 50, replicated run type = cross-validate.

The distribution of the species (both Northern and Southern lineages combined) was modeled for current time and projected into the mid-Holocene (6 kya) and the LGM (21kya) climate scenarios. The current SDM was initially built from the 19 standard bioclimatic variables from WORLDCLIM 1.4 (Hijmans et al. 2005). Environmental layers were reduced to Nicaragua, Costa Rica and Panama (12.850°N, 87.611°W by 6.558°N, 76.251°W, an area about 30 % larger than the known range). Bioclimatic variables that contributed 5 % or greater to the initial model were included in the final model. The last glacial maximum (LGM) and mid-Holocene climate layers were derived from the Paleoclimate Modelling Intercomparison Project Phase II (Braconnot et al. 2007). Given computational restrictions that limit the study area to 10,000 unique pixels for the demographic

component of the analyses, we focused on a region encompassing the southeastern border of Costa Rica, southward to the Bocas del Toro archipelago in Panama (9.762°N, 82.939°W by 7.787°N, 81.491°W) and used a pixel resolution of 0.00833 (about 1 km^2).

Ancestral distribution estimates

To estimate the ancestral distributions of populations of *O. pumilio* we used two methods: a molecular-evolutionary method to estimate centers of origin of clades and a climate-based geospatial method to estimate historic distributions. The molecular-evolutionary estimate of clade origin was performed using the continuous phylogeographical analyses (Homogeneous Continuous Diffusion model) (Lemey et al. 2010) implemented in the software Beast 1.7 (Drummond et al. 2012). The analysis consists of an ancestral reconstruction of continuous traits where geographical coordinates of the leaves of the tree are used to reconstruct the geographical coordinates of the nodes. We estimated the center of origin of *O. pumilio* using 259 *Cytochrome-b* sequences generated by Hauswaldt et al. (2010) available on Genbank (accession numbers: GQ980333–GQ980855). Geographical coordinates were retrieved from the same study. Here and in all subsequent phylogenetic analysis we estimated the substitution model using Akaike Information Criteria (AIC)(Akaike, 1974) through the software jModelTest0.1.1(Posada 2008). We ran a MCMC 108 steps long using a Tamura Nei substitution model with Gamma heterogeneity (TN93+G) and codon partitioning, an uncorrelated lognormal relaxed clock model and a fixed substitution rate of 1.54 %/site/Ma derived from the estimation procedure described below. A maximum credibility tree was summarized using TreeAnnotator 1.7.2 (Drummond et al. 2012) and imputed in the program SPREAD (Bielejec et al. 2011) which generates a graphical image of the phylogeographical reconstruction. The image is composed of branches that represent the tree and polygons that represent the 80 % high posterior density of the node traits (geographical coordinates). We assumed the polygon that corresponds to the root of the tree represents the geographical origin of *O. pumilio*.

The climate-based ancestral distribution estimate was inferred from the LGM and mid-Holocene SDMs. As implemented, we assume that the ecological niche and dispersal capabilities of *O. pumilio* have not changed since the LGM. Given that closely related taxa utilize similar habitats and demonstrate little ecological divergence, there is no reason to think that these are unreasonable choices as focal taxa.

Bayesian skyline plots

To estimate change in population size through time we performed a Bayesian Skyline Plot (BSLP) analysis using the software Beast 1.7. (Drummond et al. 2005; Drummond and Rambaut 2007). *Cytochrome b* sequences of 259 samples generated by Hauswaldt et al. 2010 (GenBank accession numbers: GQ980333–GQ980855) were used here. Two analysis were carried out, one for the Southern lineage (localities 12–24, see Hauswaldt et al. 2010 for details), and one for the Northern lineage (localities 1–8 from Hauswaldt et al. 2010). Exploratory analyses were carried out assuming a TN93+G model of substitution and uncorrelated lognormal relaxed clock, using both linear and a stepwise BSLP models with 5 and 10 groups. Both BSLP models with 5 and 10 groups yielded similar results, whereas the 5 groups BSLP showed higher values of Effective Sample Size (ESS) for the demographic parameters (data not shown). For both lineages the posterior distribution of the standard deviation of the molecular clock (*ucld.stdev* parameter) included zero (data not shown). Based on these preliminary results we performed a final analysis assuming a

stepwise BSLP model with five groups and a strict molecular clock model. We ran the MCMC for 10^8 steps sampling every 1,000 steps which was sufficient to ensure values of ESS were at minimum 200,000 for all parameters. To calibrate the BSLP we used a fixed substitution rate which was calculated following the methods described below. For each lineage we ran the final analysis 3 times with different seed numbers, and we used Tracer 1.5 (Rambaut and Drummond 2009) to check for mixing of parameter sampling and convergence among runs.

Substitution rate estimation

In order to calibrate the BSLP, the phylogeographical analysis and the genetic simulations, we estimated a substitution rate for *Cyt-b* of dendrobatids, which was subsequently used for a co-estimation of the substitution rate of *RAG-1* in *O. pumilio*. *Cytochrome b* sequences of 54 dendrobatid species were downloaded from GenBank (accession numbers HQ290530–HQ290583). The sequences were aligned with the *O. pumilio* sequences used in the BSLP analysis and non-overlapping regions were excluded in order to ensure that fragments of the same length were used in the BSLP and in substitution rate estimation. We used the resulting alignment to perform a time calibrated phylogenetic analysis, using three node constraints derived from Santos et al. (2009) in the software Beast 1.7 (Drummond and Rambaut 2007): (1) the divergence between *Dendrobates truncatus* and *Dendrobates auratus* was constrained with an uniform prior with an upper limit of 4 MYA; (2) the divergence between *Hyloxalus sauli* and *Hyloxalus bocagei* was constrained with a uniform prior with limits between 5 and 15 MYA; 3) the root was constrained with a normal prior with a mean of 43 MYA, and a standard deviation of 6.9 MYA. The estimated substitution model according to jModelTest0.1.1 (Posada 2008) was GTR with invariant sites and Gamma heterogeneity. However when applying this model we observed poor chain mixing with low values of ESS for the *prior* and *posterior*. Because over-parameterized models can cause poor chain mixing we decided to simplify the substitution model; therefore we used a HKY model with invariant sites and Gamma heterogeneity. When applying the latter model we observed fast chain mixing, stationarity was reached after approximately 20×10^4 steps, and values of ESS higher than 200,000 were reached after 10^7 steps. Given these results we ran the final MCMC for 10^8 iterations using a HKY+I+G substitution model, a Yule speciation prior and an uncorrelated lognormal relaxed clock model. We ran the analysis three times with different seed numbers and we used the software Tracer 1.5 (Rambaut and Drummond 2009) to check for mixing of parameter sampling and convergence among runs. We combined the three runs and we used the resulting median value of the *ucld.mean* parameter as an estimate of the substitution rate for the *Cyt-b* gene of dendrobatids.

Further, we performed multi-locus analysis using Beast 1.7 to co-estimate a substitution rate for the *RAG-1* gene of *O. pumilio*. For this we used all *Cyt-b* and *RAG-1* sequences of *O. pumilio* generated by Hauswaldt et al. (2010). We fixed the substitution rate of the *Cyt-b* gene to the value previously estimated and let the program co-estimate a substitution rate for the *RAG-1* fragment. We used a HKY substitution rate for *RAG-1* and a HKY+I+G for the *Cyt-b* data. The analysis was performed using a Yule speciation prior, with strict clock model for *RAG-1* and lognormal relaxed clock for the *Cyt-b* sequences. The MCMC was run for 10^8 steps, sampling each 1,000 generations. We used the median value of the *clock.rate* parameter as an estimate of the mutation rate of the *RAG-1* fragment.

Translating SDMs into demographic parameters

The predicted SDMs were translated into components for use in the demographic simulations: (1) friction landscapes (F_l) and (2) as carrying capacity landscapes (K_l) (See Brown and Knowles 2012 for a detailed overview of methods and discussion of them). In brief, the SDM values were standardized for friction landscapes so that values ranged from zero to one and were then inverted. The resulting F_l, defining the relative ease of movement of individuals among demes, depicted high predicted values of habitat suitability as low friction values to dispersal. In our demographic models, the number of emigrants per generation was the result of the migration rate (m, the per generation probability that an individual moves out of a deme) and the total number of occupants (based on local carrying capacity, k, and the logistic growth parameter, r). The spatial distribution of emigrants each generation is the result of the friction values of neighboring demes. Friction and carrying capacity landscapes were created for the three time periods that climate data were available (current time, 6 kya, 21 kya).

We used two mathematical transformations to convert the SDM into K_l and F_l: a linear conversion and a sigmoid conversion. Different transformations were considered because they change how habitat heterogeneity and spatiotemporal variation are incorporated into the carrying capacity landscape (Brown and Knowles 2012). Maximum carrying capacity was optimized so that the total maximum population of $K_{l\text{-}21\text{kya}}$ was ca. 0.8 million and the $K_{l\text{-current}}$ was ca. 8 million (values that matched the medians from our Bayesian skyline plots). This resulted in a K_{max} of 5,000 for the linear transformations and a K_{max} of 2,000 for the sigmoid transformations. Both values agreed with rough empirical field estimates of population sizes (Pröhl and Berke 2001; Richards-Zawacki et al. 2012). For the sigmoid transformations we used a normal cumulative distribution function, where $\mu = 0.25$ (the lower 10 % of the current SDM values that corresponded to observed localities) and $\sigma = 0.18$ (1/2 the standard deviation of the current SDM values corresponding to observed locality data, see Brown and Knowles 2012 for a detailed explanation).

The climatic and paleoclimatic data used here did not incorporate sea-level changes and resulting changes in terrestrial habitats. To estimate habitat suitability in areas recently covered by sea-level rises (areas with less than 140 m of water), we converted the raster SDM file to a point shapefile. This calculation converted each pixel of the raster to point-file and using this file, we performed a tensioned spline on this layer in ArcMap 10.0 (ESRI, Redlands, CA, USA) using the following parameters: weight = 0.1, number of points = 12. In our analyses, the spline interpolated values adjacent to areas where data was lacking (such as areas below sea-level). After the spline was performed, the pre-splined habitat data were mosaicked with the splined data, selecting pre-splined habitat data for cells with data and filling in the splined data where raw data was absent.

Spatially explicit models of dynamic histories

Creating temporally continuous landscapes for demographic simulations

The SDMs provide predictions for time-specific periods for past and current distributions, separated by thousands of years, and do not predict a continuous transition from past to current time periods. As a basis for inferring the rate and timing of climate change history in the northern hemisphere, we used oxygen isotope ratios from Greenland ice core samples that are available at a fine temporal scale (Andersen et al. 2004). To estimate K_l

and F_l for time periods lacking climate data, we approximated climate change (based on oxygen isotope ratio data) between the three periods where bioclimatic data is available and then based on this simplified scenario, interpolated the data between temporally adjacent K_l (or F_l, see Brown and Knowles 2012 for a detailed explanation).

Demographic and genetic simulations

A demographic colonization process was simulated based on growth, migration and density limitations imposed by the environment (the F_l and K_l landscapes) using SPLATCHE 2 (Ray et al. 2010). These simulations were performed from past to current conditions, with the colonization of contemporary populations dependent upon the demographic and environmental parameters. To examine the genetic consequences of the distributional shifts, coalescent genealogies parameterized by the spatially explicit demographic conditions were simulated and genes were sampled from focal populations (See Brown and Knowles 2012 for an overview of data flow and input parameters; Excoffier et al. 2000; Currat et al. 2004; Ray et al. 2010).

For the genetic simulations we focused on conditions that correspond to empirical data sets with both nuclear and mitochondrial genetic data available (from Hauswaldt et al. 2010). Specifically, all the simulated genetic data matched the empirical data with respect to the number of individuals and spatial distribution, the number of loci sequenced, number of base pairs per locus and corresponding model of nucleotide evolution. The genetic data simulated for this study corresponded to the empirical data consisting of 572 bp of mtDNA (*cytochrome b* gene) and 581 bp of nDNA (*RAG-1* gene) for 156 individuals (consisting of 301 unique haplotypes) from 15 populations (Table 2).

Genetic data were simulated using sequence transition–transversion rates estimated in MacClade 4 (Maddison and Maddison 2005); rates of recombination were set to 0.822 cM/Mb for nDNA (based on an average of vertebrate autosomal recombination rates, see Dumont and Payseur 2008) and zero for mtDNA. For the genetic simulations, we used a mtDNA substitution rate of 0.0155 nucleotides per gen. and a nDNA mutation rate of 0.00096 nucleotides per gen. estimated specifically for our dataset (see above). The following parameters were considered in the demographic simulations: growth rate of 4 (proportional increase per gen.) (Donnelly 1989; Brust 1993); migration rates between 0.001 and 0.1 km/year (estimated from Wang and Summers 2010) and 11,000 generations (1 generation = 2 years). The generation time is a limitation imposed by the simulations and, currently, a smaller value cannot be achieved for our analyses. To account for a doubled generation time, the mutation rate was multiplied by 2 in simulations. Initial population densities in the demographic model were obtained from a modified LGM SDM (linear transformed with K_{max} of 2,000), where the presence of marine introgression and SDM values below 0.3 were converted to zero. This initial distribution was corroborated with the LGM ancestral distribution estimates (discussed above).

For each set of demographic conditions, ten demographic simulations were performed (summarized in Table 3) and within each demographic simulation, ten replicate genetic simulations were performed (totaling one hundred genetic simulations per parameter set).

Evaluating the impact of demographic model parameters

To evaluate how similar the simulated values were to those observed in the empirical genetic data, we considered a number of summaries of genetic variation calculated across

Table 2 Focal population, locality names, abbreviation, coordinates and number of individuals of *O. pumilio*

#	Locality	Abb.	Region	Country	Latitude (N)	Longitude (W)	Number of individuals
1	Bribri	CRB	South-eastern CR	CR	9.64547	−82.88258	9
2	Puerto Viejo de Talamanca	CRTB	South-eastern CR	CR	9.64756	−82.75619	11
3	Almirante	PAA	Bocas del Toro	PA	9.2861	−82.39065	9
4	Tierra Oscura	PAT	Bocas del Toro	PA	9.17893	−82.25878	8
5	Cauchero	PAK	Bocas del Toro	PA	9.15642	−82.25432	12
6	Colón	PAC	Bocas del Toro	PA	9.38652	−82.23623	12
7	Bastimentos	PAB	Bocas del Toro	PA	9.30361	−82.14028	10
8	Solarte	PAS	Bocas del Toro	PA	9.33263	−82.21855	10
9	San Cristobal	PASC	Bocas del Toro	PA	9.27152	−82.29005	9
10	Pastores	PAPA	Bocas del Toro	PA	9.23992	−82.35055	9
11	Popa	PAP	Bocas del Toro	PA	9.215	−82.12978	18
12	Loma Partida	PAL	Bocas del Toro	PA	9.13645	−82.16513	10
13	Cayo de Agua	PACA	Bocas del Toro	PA	9.1574	−82.04888	12
14	Punta Alegre	PA	Bocas del Toro	PA	9.16333	−81.90921	8
15	Escudo de Veraguas	PAE	Escudo de Veraguas	PA	9.10177	−81.54932	9

all populations: the number of pairwise nucleotide differences (p), heterozygosity, number of segregating sites, number of private polymorphic sites (PPS, the number of polymorphic sites unique to each population) and F_{ST} (based on genetic distances from a Tamura and Nei substitution model). All genetic calculations were performed in ARLSUMSTAT and ARLEQUIN 3.5.1.2 (Excoffier and Lischer 2010). Due to significant correlation among some summary statistics, a standardized principal component analyses (PCA) was performed reducing the data to 3 principal components (PCs).

Relative differences in the match between simulated and observed genetic data across models

Mean principal component values between each scenario and the observed genetic data were compared. Confidence intervals ($\alpha = 0.05$) of PC values were calculated in SPSS v.15 for each scenario and used to measure statistical significance of differences between simulated values compared to the PC values of observed molecular data.

Selection on coloration, sea-level rise and population expansion

To estimate the potential role of recent population expansion and isolation resulting from sea-level rise on the evolution of coloration, we created four demographic scenarios (S1–S4, Fig. 2) that either possessed a dynamic or static climate and either a dynamic or

Table 3 Analyses of how similar the simulated values were to those in the empirical observed genetic data

Simulation parameters			Principal component values: mean (95 % CI)		
m	Scenario	Transformation	PC1	PC2	PC3
0.001	S1	Linear	0.991 (1.134 to 0.847)	−0.247 (−0.055 to −0.439)	0.024 (0.523 to −0.475)
0.01	S1	Linear	−0.351 (−0.245 to −0.458)	0.281 (0.457 to 0.105)*	−0.270 (0.292 to −0.832)
0.1	S1	Linear	−0.973 (−0.890 to −1.057)	0.757 (0.929 to 0.585)	0.383 (0.996 to −0.230)
0.001	S2	Linear	0.228 (0.375 to 0.080)	−0.636 (−0.467 to −0.805)	−0.289 (0.288 to −0.866)
−0.01	S2	Linear	−1.005 (−0.913 to −1.096)	−0.098 (0.006 to −0.203)	−0.504 (−0.146 to −0.861)
0.1	S2	Linear	−1.538 (−1.475 to −1.602)	0.123 (0.214 to 0.031)*	0.385 (0.855 to −0.086)
0.001	S3	Linear	0.696 (0.828 to 0.565)	−0.777 (−0.593 to −0.961)	−0.227 (0.252 to −0.706)
0.01	S3	Linear	0.186 (0.217 to 0.155)	−0.212 (−0.112 to −0.312)	−0.833 (−0.300 to −1.365)
0.1	S3	Linear	−0.410 (−0.324 to −0.496)	0.025 (0.187 to −0.138)*	−0.694 (−0.078 to −1.310)
0.001	S4	Linear	0.154 (0.301 to 0.007)	−0.881 (−0.702 to −1.061)	−0.221(0.318 to −0.759)
0.01	S4	Linear	0.040 (0.052 to 0.028)	−1.303 (−1.230 to −1.375)	−0.144 (0.374 to −0.662)
0.1	S4	Linear	−1.923 (−1.853 to −1.994)	−0.556 (−0.463 to −0.650)	1.045 (1.589 to 0.501)*
0.001	S1	Sigmoid	1.868 (2.047 to 1.689)*	−0.249 (−0.050 to −0.448)	0.739 (1.247 to 0.231)*
0.01	S1	Sigmoid	0.238 (0.342 to 0.134)	0.478 (0.682 to 0.275)	−0.248 (0.257 to −0.753)
0.1	S1	Sigmoid	−0.510 (−0.414 to −0.605)	1.103 (1.301 to 0.904)	0.331 (0.865 to −0.203)
0.001	S2	Sigmoid	1.048 (1.258 to 0.839)	−0.641 (−0.265 to −1.016)	0.332 (0.823 to −0.160)
0.01	S2	Sigmoid	0.591 (0.713 to 0.470)	2.264 (2.493 to 2.035)	−0.132 (0.421 to −0.685)
0.1	S2	Sigmoid	0.406 (0.530 to 0.282)	2.689 (2.945 to 2.434)	0.027 (0.517 to −0.462)
0.001	S3	Sigmoid	1.581 (1.727 to 1.435)	−0.922 (−0.708 to −1.135)	0.560 (1.026 to 0.095)
0.01	S3	Sigmoid	0.230 (0.338 to 0.123)	−0.202 (−0.041 to −0.364)	−0.795 (−0.227 to −1.364)
0.1	S3	Sigmoid	−0.156 (−0.060 to −0.251)	0.050 (0.198 to −0.097)*	−0.849 (−0.331 to −1.367)
0.001	S4	Sigmoid	0.985 (1.155 to 0.816)	−0.799 (−0.591 to −1.007)	0.299 (0.789 to −0.192)

Table 3 continued

Simulation parameters			Principal component values: mean (95 % CI)		
m	Scenario	Transformation	PC1	PC2	PC3
0.01	S4	Sigmoid	−0.937 (−0.843 to −1.032)	−0.699 (−0.564 to −0.834)	−0.058 (0.585 to −0.701)
0.1	S4	Sigmoid	−1.778 (−1.726 to −1.831)	−0.571 (−0.476 to −0.666)	0.757 (1.238 to 0.277)*
Observed genetic values			1.998	0.115	1.154

Principal component analyses of genetic variation were calculated across all populations on the following summary statistics: the number of pairwise nucleotide differences, heterozygosity, number of segregating sites, number of private polymorphic sites and F_{ST}. The first, second and third components represented 54.2, 11.8, 4.0 % of the observed genetic variation. Mean principal component values of parameter sets and 95 % CI in parentheses

* Simulations that matched the observed empirical genetic values (within the 95 % CI of the simulation)

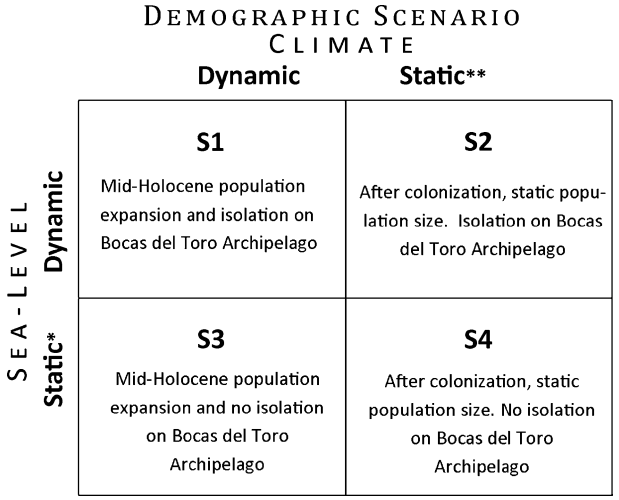

Fig. 2 Four demographic scenarios and the population consequences resulting from the inclusion of static or dynamic sea-level and static or dynamic climate. *Static sea-level = sea-level of LGM (140 m below current levels) **static climate = current climate

static sea-level. If a static climate was used, it was derived from the current climate data and this resulted in no mid-Holocene population expansion. If a static sea-level was used, the sea-level was fixed at LGM levels and this resulted in no marine introgression into the Bocas del Toro archipelago, thus no populations became isolated on islands.

We measured the level of similarity between a neutrally evolving nuclear gene in each population and then compared that to the deep coalescence of a hypothetical autosomal coloration gene (based on the observed coloration of each population). Slatkin and Maddison's *s*, a test statistic that counts the number of changes of a character corresponding to population membership, was used to summarize discordance between genetic and population data (Slatkin and Maddison 1989). In other words, Slatkin and Maddison's *s* measures the discord between coloration (the character used in this study) and population membership. Our population tree was based primarily on the topology of Wang and Shaffer (2008). Only a single population tree was used because Slatkin and Maddison's *s* value is not sensitive to overall tree topology and only the population relationships are considered when calculating *s* (as opposed to accounting for branch lengths and overall

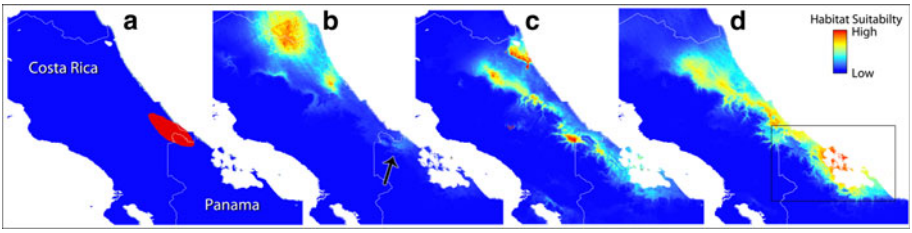

Fig. 3 Map of estimates of ancestral distributions. **a** Molecular estimate of the distribution to most recent common ancestor of focal populations, *red area* depicted represents the 80 % high posterior density of the node traits (geographical coordinates) and represents the likely center the origin of the most recent common ancestor of *O. pumilio* "S". Bioclimatic estimates of distribution of *O. pumilio* during the **b** last glacial maximum, **c** mid-Holocene and **d** current time. *Warmer colors* higher habitat suitability. The LGM and mid-Holocene SDMs had much lower maximum suitability scores (0.573 and 0.679, respectively) than the current SDM (0.926). *Black box* area of demographic and genetic simulations. (Color figure online)

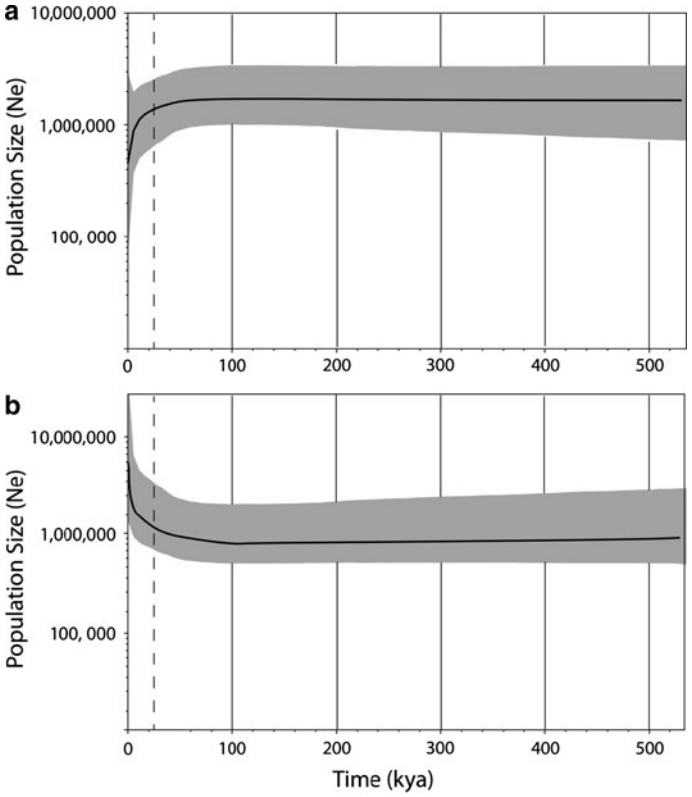

Fig. 4 Bayesian skyline plots of Northern and Southern lineages of *O. pumilio* displaying effective population sizes plotted as a function of time. The time scale begins with present on the left. *Black lines* the median value of effective population sizes. *Grey areas* the 95 % posterior probability interval. The last glacial maximum is depicted by the *dashed vertical line*

tree topology as in other measures of deep coalescence). Thus uncertainties in the explicit topology of a population phylogeny (relationships among populations) have no consequence for the resulting *s*-values (Slatkin and Maddison 1989).

Coalescent genealogies parameterized by the four demographic scenarios (Fig. 2) were simulated and nuclear genes were sampled from the 15 focal populations. Each parameter set resulted in 115,300 simulated gene trees. Values of *s* were calculated for each tree and the distribution of *s*-values was used to estimate confidence intervals ($\alpha = 0.05$). To estimate the *s*-value for a hypothetical color gene, we measured the *s*-value for 15 monophyletic populations (using the population tree above). We acknowledge that there is some geographic structuring of island phenotypes and that the color morphs are not randomly distributed. However, because all the phenotypes of focal populations have diverged from all others in some manner, we think this was an appropriate assumption (Maan and Cummings 2012). We can reject the neutral evolution of coloration if the *s*-values of the hypothetical coloration scenario fall outside the CI of the demographic scenario. The greater the differences in *s*-values of the hypothetical color gene and each demographic scenario, the greater the likely role of selection in the evolution of coloration.

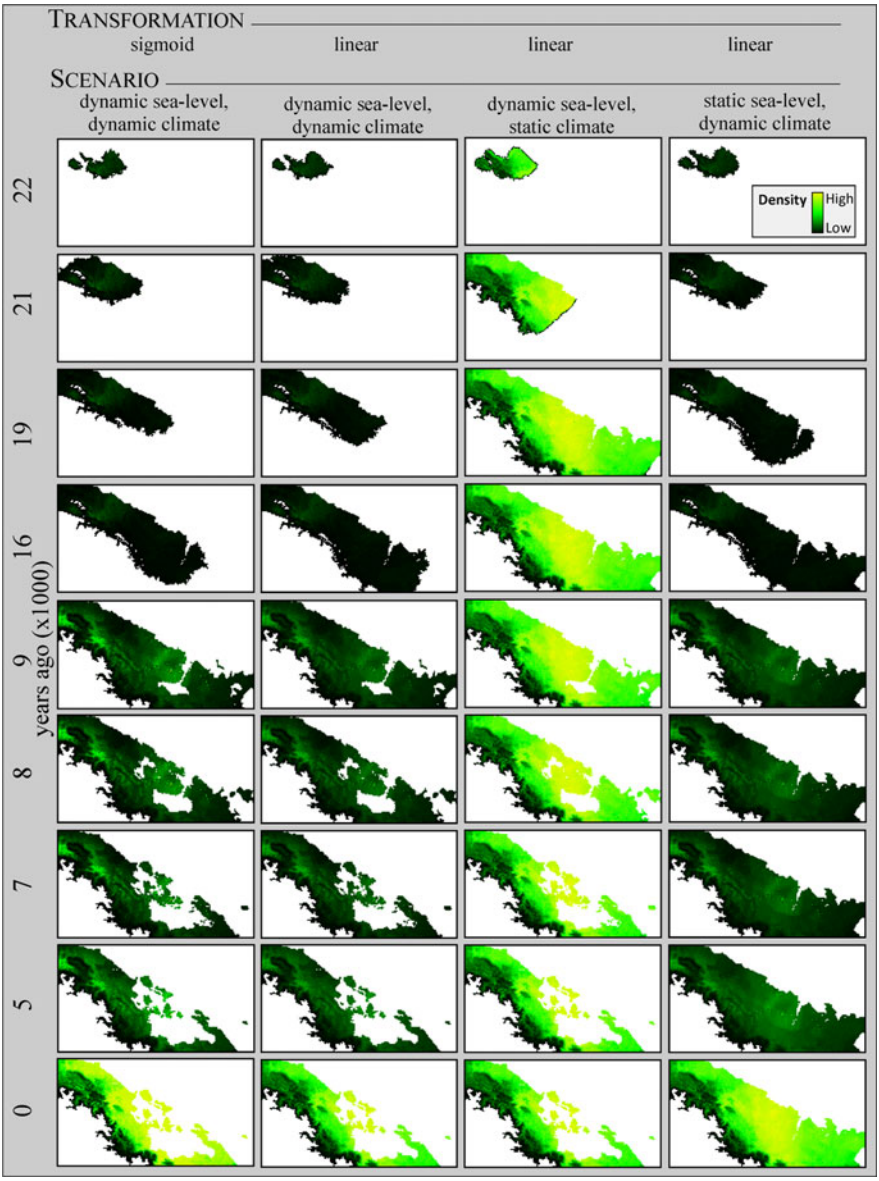

Fig. 5 The impact of different transformation types on the distribution of populations through time. The *columns* represent different combinations of transformation type and demographic scenario. The *rows* depict changes in distributions/densities through time from LGM to current time (*top* to *bottom*). *Bright yellow colors* depict higher population densities and *darker colors* represent lower densities. Areas unoccupied at that time period are *white*. All examples depict a population expanding southward into the Bocas del Toro archipelago. In simulations that included dynamic sea-level, the sea level dramatically rises around 16 kya creating many of the islands that occur in the Bocas del Toro archipelago. The data shown were simulated with $m = 0.001$. See Fig. 3 for a map of the area contained in the simulations. *Note* static climate and sea-level scenario (*not pictured*) appears very similar to the dynamic sea-level and static climate scenario during time periods 22–16 kya. The static seal-level and static climate distribution during time periods 16–0 kya appears identical to 16 kya distribution of the dynamic sea-level and static climate scenario. (Color figure online)

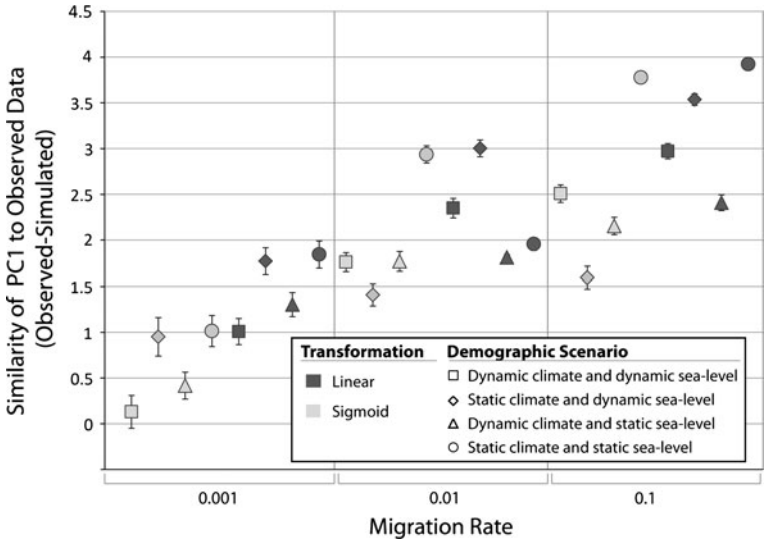

Fig. 6 Comparison of impact of different demographic models on patterns of genetic variation by PC1 (representing 54.2 % of the genetic variation) characterized for each population: the number of pairwise nucleotide differences (*p*), heterozygosity (*He*), number of segregating sites, number of private polymorphic sites (PPS) and F_{ST}. *Values* represent the PC1 of simulated data subtracted from the PC1 value of the observed genetic data, hence *values closer* to *zero* represent scenarios that best match the observed genetic data. Migration rate (the per generation probability that an individual moves out of a deme) was a major contributor to PC1 values. The scenarios with $m = 0.001$ resulted in values most similar to the empirical dataset. These results support the inference that migration was low for *O. pumilio*. A single scenario (transformation = sigmoid, $m = 0.001$, scenario = dynamic climate and dynamic sea-level) was not rejected by the 95 % CI

Results

Ancestral distribution estimates

The molecular estimate of the ancestral center of origin of the *O. pumilio* "S" mitochondrial lineage place the distribution around the border between Costa Rica and Panama on the eastern versant of the Cordillera Talamanca (Fig. 3a). The climatic estimate of LGM ancestral distributions place the core of this lineage's distribution near the border of Costa Rica and Nicaragua on the east versant of Cordillera Talamanca (Fig. 3b) and a secondary area predicted near the border between Costa Rica and Panama on the eastern versant of the Cordillera Talamanca (agreeing with the molecular estimate). The SDM of the mid-Holocene predicted the distribution to be similar to the contemporary distribution (Fig. 3c, d); however the areas of highest suitability are centered in the higher elevations (vs. low elevations). The LGM and mid-Holocene SDMs had lower maximum suitability scores (0.573 and 0.679, respectively) than the current SDM (0.926).

Bayesian skyline plots

The Bayesian Skyline Plots revealed a complex demographic history. The Northern *O. pumilio* displayed a negative trend in median effective population since approximately

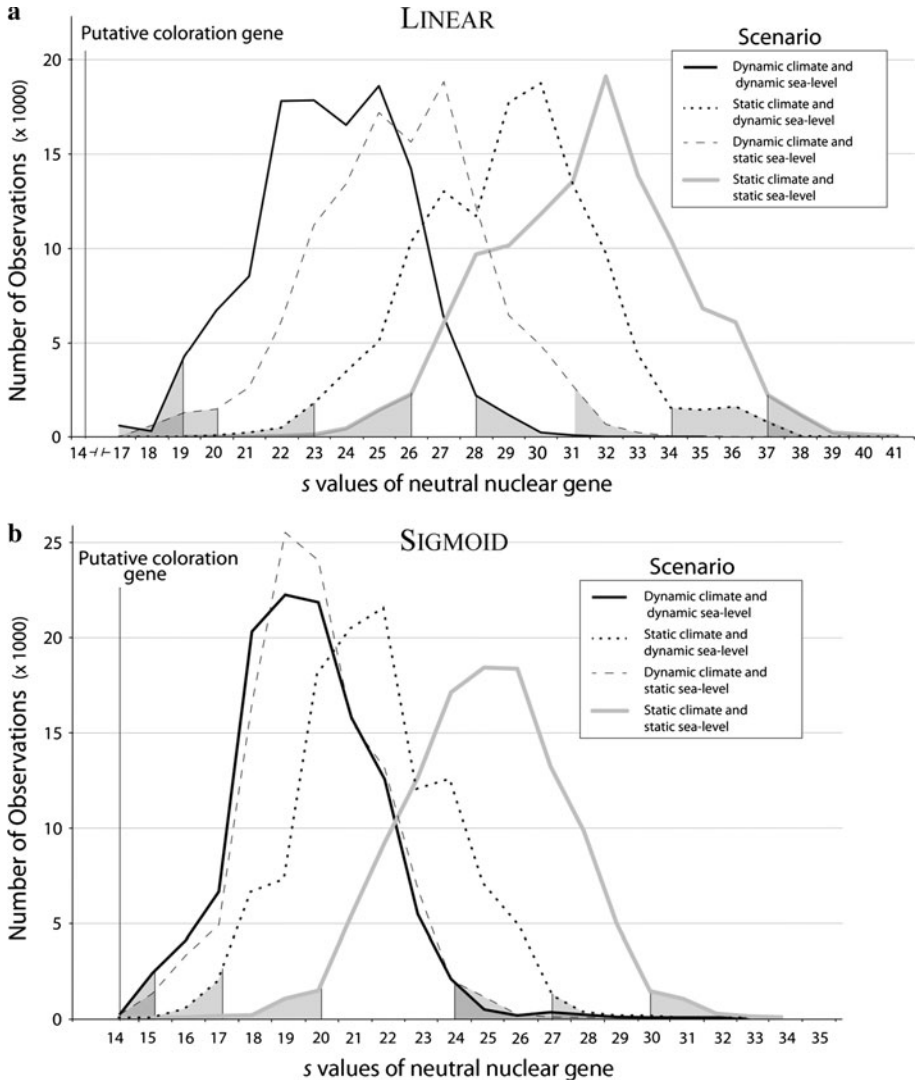

Fig. 7 Similarity between a neutrally evolving nuclear gene and each population compared that to the *s* of a hypothetical autosomal coloration gene. Slatkin and Maddison's *s* counts the number of changes of a character corresponding to population membership and was used to summarize discordance between genetic and population data (Slatkin and Maddison 1989).We measured *s*-values for all simulations with $m = 0.001$ due to their similar genetic values. *Values* of *s* are represented for each transformation: linear (**a**) and sigmoid (**b**) for the four demographic scenarios. If *s*-values of simulations equal that of the hypothetical autosomal coloration gene, the evolution of coloration can be explained by neutral demographic processes and does not require selection. The greater difference in *s*-values of a hypothetical coloration gene and simulated values, the greater the intensity of selection required for the evolution of novel coloration. *Shading* depict areas outside the 95 % CI (rounded to up or down to nearest integer for lower and upper distributions, respectively)

50 kya (Fig. 4a). Considering the confidence intervals, we cannot, however, exclude the possibility of stable population size through time. In contrast, the Southern *O. pumilio* lineage exhibited a signature of recent population expansion (of approximately one order

of magnitude) in the last 50ky (Fig. 4b). It is possible that the date of the demographic changes are underestimated, given that the substitution rate used could represent an underestimation of the spontaneous mutation rate that happened at population level, artificially pulling recent nodes to the past (Ho et al. 2005, 2011). However, assuming that the calibrations used in the substitution rate estimation are correct, it is unlikely that the time of the demographic change is underestimated (Grant et al. 2012). Therefore it is reasonable to assume that the demographic changes happened as or more recently than 50 Ky.

Spatially explicit models of dynamic histories

Only a few demographic models produced values that were similar to the observed genetic values (Table 3). Here we present the results of the first three principal components that represented 70.0 % of the total genetic variation (54.2, 11.8, 4.0 %, respectively). In PC1, a single scenario (sigmoid transformation where $m = 0.001$, S1) was not rejected at the level of the 95 % CI (Figs. 5, 6). For PC2, four scenarios produced values similar to the observed genetic data and were not rejected at the level of the 95 % CIs (linear transformation: $m = 0.1$, S2; $m = 0.1$, S3; $m = 0.01$, S1; and sigmoid transformation where $m = 0.1$, S3). However several other parameter sets produced values similar to those observed (Table 3). For PC3, three scenarios produced values similar to the observed genetic data and were not rejected at the level of the 95 % CI (linear transformation where $m = 0.1$, S4; and sigmoid transformation: $m = 0.001$, S1; $m = 0.1$, S4).

Selection on coloration, sea-level rise and population expansion

The *s*-value of a hypothetic autosomal color gene is 14 (the lowest possible value given the number of populations), a value outside of the 95 % confidence intervals of all simulations. The four demographic scenarios resulted in different distributions of *s*-values (Fig. 7). Under the linear transformation, no scenario produced values as low as 14 (Fig. 7a). Mean (min–max) values for each scenario of the linear transformation are: S1, 23.56 (17–31); S2, 29.03 (20–39); S3, 25.69 (18–35); S4, 31.44 (19–41). In the sigmoid transformation, two scenarios (S1 and S2) produced *s*-values of 14 (Fig. 7b). Mean values (min–max) for each scenario of the sigmoid transformation are: S1, 19.65 (14–29); S2, 21.73 (16–30); S3, 19.85 (14–28); S4, 25.02 (16–34).

Discussion

Deep coalescence and demographic scenarios

Scenarios that incorporate a dynamic (vs. static) climate, resulting in a mid-Holocene population expansion, had the lowest mean *s*-values (linear dynamic climate 24.63 vs. linear static climate 30.23; sigmoid dynamic 19.75 vs. sigmoid static 23.37). Dynamism in sea-level (resulting in isolation of populations on islands in the Bocas del Toro archipelago) also reduced *s*-values, however to a lesser degree than dynamic climate (Fig. 7). In the linear transformation, the difference of mean *s*-values between S4 and S3, or S4 and S2 were 5.75 and 2.41, respectively. These results suggest that recent population expansion resulted in faster coalescent rates than isolation on islands and therefore, would have a greater effect on a demes' response to selection. However, the inclusion of both dynamic

scenarios had an additive effect on the deep coalescence total (*s*-values) in the linear transformation, supporting the notion that both contribute to a population's response to selection. In S1, the difference between it and S4 was 7.88 (the sum of differences between S1 and S3, and S1 and S2 were 8.16). Independent contributions of dynamic sea-level and dynamic climate were not as defined in the sigmoid transformation. This was, in part, because S1 and S3 produced *s*-values near the lowest value possible in our simulations ($s = 14$) and because of this, differences between the two likely did not matter. The two scenarios that included dynamic climate (S1 and S3) produced mean s-values that were almost identical (19.65 vs. 19.85), S2 produced *s*-values intermediate between S1/S3 and S4. These results demonstrate that the distinct demographic scenarios resulted in different levels of deep coalescence, and because of this, could dramatically affect a population's response to divergent selection.

Similarity between simulated data and empirical data

With regard to the suite of conditions and demographic models considered here, several resulted in PC values that closely matched the observed genetic values and fell within the 95 % CI of a simulation parameter set. Most notably, S1 of the sigmoid transformation produced genetic values that matched the observed values in PC1 and PC3 (Fig. 6; Table 1). No other parameter set matched the observed genetic values in PC1, which represented 54.2 % of the measured genetic variation. Conversely, few scenarios produced genetic values that fell within the 95 % CI of any of the first three PCs. This demonstrates that even with the limited set of summary statistics considered here, many modeled scenarios can be considered highly unlikely and statistically rejected as possible representations of the true demographic history.

Demography and the evolution of coloration in *O. pumilio*

Our results suggest substantially different roles for natural selection (compared to previous treatments) in the evolution of coloration. In a static environment, very strong selection is required to produce similar diversity in coloration, whereas the scenario that emulated the likely history of *O. pumilio* "S" (in a dynamic environment with improving climate and isolation of populations on the Bocas del Toro Archipelago islands) entails a reduced role for diversifying selection (although selection is still required). These results are concordant with those of Brown et al. (2010), in which sequences were simulated under a fixed population size; however, here we infer a reduced need for selection due to the fact that we simulated genealogies based on more realistic spatiotemporally explicit models. Although the two scenarios resulted in values that matched the hypothetical coloration gene (albeit outside the 95 % CI), these scenarios do not provide a specific reason why coloration would diverge substantially among populations. Thus, in the absence of diversifying selection (such as sexual selection), demographic processes are unlikely to entirely explain the observed divergence in coloration. However as demonstrated here, historical demography dramatically influences the strength of selection required for populations to diverge. These simulations shed light on the disparity in color variation between the two *O. pumilio* lineages (Northern and Southern), which have experienced dramatically different demographic histories (as opposed to differences in the genetics of coloration, and female mate choice). *Oophaga pumilio* "N" experienced a recent population decline, causing rapid range contractions, but maintained some population connectivity (Wang and Summers 2010). These factors can increase local genetic diversity by decreasing coalescent rates

(Excoffier et al. 2009; Arenas et al. 2012), and, as a result, require a much greater role for selection for local color divergence. Thus, even if the intensity of sexual selection and natural selection remained constant through time and space, demographic processes could dramatically change the effect of both on local phenotypes.

Our results support a major role for recent population expansion in the diversification of color diversity in addition to natural selection and female mate choice. These results do not rely on drift due to small population sizes to initiate color divergence, but population expansion and possibly gene surfing, resulting in intense genetic drift taking place at the edge of the expanding population front. In our simulations we cannot distinguish between the signatures of drift from population expansion and gene surfing, however the recent divergence of *O. pumilio* "S" almost perfectly matches conditions known to favor gene surfing (see Excoffier et al. 2009). These results also support a role for reduced gene flow from isolation on islands because it reduces the strength of selection required, particularly early in the evolution of different color morphs. Recent estimates of gene flow from microsatellite analyses (Wang and Summers 2010) also match this pattern, where researchers found high levels of gene flow among the Northern populations and extremely low levels of gene flow among Southern populations. However, geographic isolation does not appear to be required for color divergence (see Sigmoid S3) and several adjacent mainland localities also contain divergent color morphs, despite being part of generally contiguous tracts of suitable habitat.

Evaluating other hypotheses

Many major hypotheses of color divergence in *O. pumilio* "S" are not mutually exclusive and most invoke a role for sexual selection, thus it can be difficult to distinguish among them with currently available data. One method is to evaluate which hypothesis best explains the observed levels of phenotypic variation in light of key biological, demographic and spatial differences among each lineage (as relevant to major mechanisms invoked in each hypotheses). Some of these hypotheses were developed only in the context of the Bocas del Toro populations. However in light of similar (or identical) natural history, mating systems and genetic composition (due to recent shared common ancestry), we expand these hypotheses to all populations of *O. pumilio*. The following are key differences among lineages: genetic diversity (e.g., Hauswaldt et al. 2010); alkaloid profiles (Saporito et al. 2007; Maan and Cummings 2012), bioacoustic parameters (Pröhl et al. 2007), predation pressures (Hegna et al. 2012), behavioral (sexual, anti-predator and feeding behaviors) (Rudh et al. 2011; Pröhl and Ostrowski 2011), recent demography (this study), gene flow between populations, and the level of population isolation (Wang and Summers 2010).

Indicator of toxicity

Large differences in toxicity among lineages could lead to significant differences in natural selection and subsequently change the influence sexual selection has on local coloration (particularly in small populations). A recent study (Hegna et al. 2012) demonstrated that predation pressure varies between a mainland population and Isla Colón, an island within the Bocas del Toro archipelago. Further, other studies have demonstrated that individuals with more contrasting coloration (red phenotypes), when compared to more cryptic coloration (green phenotypes) differ in their sexual, anti-predator and feeding behaviors (Rudh et al. 2011; Pröhl and Ostrowski 2011). These observations are consistent with the hypothesis that variation in dorsal coloration is mediated by an interaction between natural

selection by predators and sexual selection by female mate choice. Female choice likely causes locally adapted coloration favoring specific phenotypes. Depending on predators, alkaloid availability in local prey and local background, this may allow for variation in hue without loss of the aposematic signal in situations where aposematism is an honest indicator of toxicity or selection for crypsis in cases where toxicity is reduced (Maan and Cummings 2012). The concept of honest signaling of aposematism remains highly contentious. Wang (2011) demonstrated in a closely related species, *Oophaga granulifera*, that toxicity and conspicuous coloration among morphs of this species were inversely related. Another study on poison frogs of the genus *Ameerega* similarly concluded that the strength of aposematic signal was inversely related to their toxicity (Darst et al. 2006).

Another factor related to the indicator of toxicity hypothesis that needs to be further investigated is how temporal and spatial variation of toxicity affects the evolution and maintenance of polytypy. Saporito et al. (2006, 2007) demonstrated that populations of both lineages of *O. pumilio* demonstrate considerable variation in alkaloid profiles through time within and between individuals of each group. They also demonstrated that the alkaloid profiles of the mainland populations (*O. pumilio* "N") vary considerably and because of this, it does not appear coloration is always an accurate predictor of toxicity (Saporito et al. 2007).

Behavioral and geographic isolation

Coalescent simulations are consistent with the hypothesis that geographic and behavioral isolation is important, supporting a role for strong diversifying selection driving divergence in coloration (Brown et al. 2010). A theoretical study on *O. pumilio* supported the plausibility of this scenario (Tazzyman and Iwasa 2010). Further, this hypothesis is also consistent with observed differences in gene flow and isolation, with mainland populations experiencing reduced isolation and increased gene flow among populations, something that is congruent with the different rates of color diversification between the two groups (Wang and Summers 2010). However, the occurrence of several novel morphs on the mainland suggest that drift due to isolation on islands alone is not the only mechanism initiating the divergence of the southern populations.

Geographic isolation

Several studies found evidence against the geographic isolation hypothesis, supporting the argument that drift acting on small populations and geographic isolation alone cannot explain the rapid diversification of *O. pumilio* "S" (Wang and Summers 2010; Brown et al. 2010; this study). Differences in genetic diversity could also potentially explain differences in color polymorphism, however in *O. pumilio* there is no apparent correlation between genetic diversity and color diversity (Hagemann and Pröhl 2007) and the Southern lineage possess considerably lower genetic diversity (vs. the Northern lineage), but contains morphs that span the visible spectrum.

Dorsal conspicuousness, coupled drift and behavioral isolation

For other hypotheses (dorsal conspicuousness, coupled drift and behavioral isolation), the observed differences between lineages were not directly applicable to major diversification mechanisms. Therefore, these hypotheses cannot explain differences in levels of color polytypism among lineages (Maan and Cummings 2009; Tazzyman and Iwasa 2010; Wang and

Summers 2010). This supports the argument that a key mechanism is missing. Nevertheless, we cannot reject a role for the proposed mechanisms, particularly in the presence of supporting data (Maan and Cummings 2009; Tazzyman and Iwasa 2010; Wang and Summers 2010).

For example, different rates of gene flow could have a dramatic influence on the rates of color diversification; however in the context of both lineages of *O. pumilio* the cause of isolation (behavioral or geographic) is important. Wang and Summers (2010) measured correlations between genetic structure, coloration and geography. They concluded that selection drove phenotypic divergences that resulted in reduced gene flow through selection against immigrant phenotypes (but mentioned no role for geographic isolation due to marine introgression on the Bocas del Toro islands). Their conclusions, in the absence of a role for geographic isolation or another unspecified mechanism, cannot explain initial differences in lineage phenotypic divergence.

Conclusions

Our results support the argument that the inclusion of spatiotemporal dynamics is important when studying the impact of distributional shifts on patterns of genetic data and diversifying selection. Demographic history can dramatically influence the level of selection required for phenotypic diversification and populations that undergo rapid population expansion require reduced levels selection to undergo divergence in phenotype. Here we have summarized the major hypotheses concerning the color diversification of *O. pumilio*, including proposing a novel hypothesis termed the Expansion and Isolation model (EIM). Almost all analyses on the evolution of coloration support a strong role for female mate choice (Summers et al. 1997; Maan and Cummings 2009; Wang and Summers 2010; Brown et al. 2010; Maan and Cummings 2012), however the exact role of other mechanisms (i.e., natural selection, isolation, drift) remain unclear. Unlike the other hypotheses, the Indicator of Toxicity (IOT) and EIM hypotheses were able to explain the different levels of color divergence among the two lineages of *O. pumilio*. The IOT hypothesis focused on spatial variation of natural selection for aposematism/crypsis corresponding to local abundances of predators and toxic prey, whereas EIM hypothesis focused on different demographic histories among the two lineages that resulted in different responses to diversifying selection from female mate choice and continued stabilizing selection for aposematism. Hence, the two hypotheses are entirely compatible with each other. Future research is needed to clarify the explicit roles of each of these factors in context of both hypotheses. It is possible, even likely, that spatiotemporal variation in both local abundances of predators and toxic prey, and localized regions of intense drift (due to recent population expansion and small island population sizes), both played important roles in the color diversification of the southern populations of *O. pumilio*.

Acknowledgments We are indebted to M. Vences and S. Hauswaldt for their support and advice on this project. This material is based upon work supported by KAAD (Katholischer Akademischer Ausländer-Dienst) Ph. D scholarship (MCG) and by the National Science Foundation Grant No. 0905905 (JLB).

References

Akaike H (1974) A new look at the statistical model identification. IEEE Trans Autom Control 19:716–723

Andersen KK, Azuma N, Barnola JM et al (2004) High resolution record of Northern Hemisphere climate extending into the last interglacial period. Nature 431:147–151

Anderson RP, Handley CO (2002) Dwarfism in insular sloths: biogeography, selection, and evolutionary rate. Evolution 56(5):1045–1058
Arenas M, Ray N, Currat M, Excoffier L (2012) Consequences of range contractions and range shifts on molecular diversity. Mol Biol Evol 29(1):207–218
Bee MA (2003) A test of the 'dear enemy effect' in the strawberry dart-poison frog (*Dendrobates pumilio*). Behav Ecol Sociobiol 54:601–610
Bielejec F, Rambaut A, Suchard MA, Lemey P (2011) SPREAD: spatial phylogenetic reconstruction of evolutionary dynamics. Bioinformatics 27:2910–2912
Braconnot P, Otto-Bliesner B, Harrison S et al (2007) Results of PMIP2 coupled simulations of the Mid-Holocene and Last Glacial Maximum–Part 1: experiments and large-scale features. Clim Past 3:261–277
Brown JL, Knowles LL (2012) Spatially explicit models of dynamic histories: examination of the genetic consequences of Pleistocene glaciation and recent climate change on the American Pika. Mol Ecol 21(15):3757–3775
Brown JL, Maan ME, Cummings ME, Summers K (2010) Evidence for selection on coloration in a Panamanian poison frog: a coalescent-based approach. J Biogeogr 37(5):891–901
Brown JL, Twomey E, Amézquita A et al (2011) A taxonomic revision of the Neotropical poison frog genus *Ranitomeya* (Amphibia: Dendrobatidae). Zootaxa 3083:1–120
Brust DG (1993) Maternal brood care by *Dendrobates pumilio:* a frog that feeds its young. J Herpetol 27(1):96–98
Bunnell P (1973) Vocalizations in the territorial behavior of the frog *Dendrobates pumilio*. Copeia 1973(2):277–284
Coates AG, Obando JA (1996) The geologic evolution of the Central American Isthmus. In: Jackson JBC, Budd AF, Coates AG (eds) Evolution and environment in tropical America. University of Chicago Press, Chicago, IL, pp 21–56
Coates AG, Collins LS, Aubry MP, Berggren WA (2004) The geology of the Darien, Panama, and the late Miocene–Pliocene collision of the Panama arc with northwestern South America. Geol Soc Am Bull 116:1327–1344
Colinvaux PA (1991) A commentary on: palaeoecological background: neotropics. Clim Change 19:49–51
Colinvaux PA, Liu K-B, de Oliveira P et al (1996) Temperature depression in the lowland tropics in glacial times. Clim Change 32:19–33
Currat M, Ray N, Excoffier L (2004) SPLATCHE: a program to simulate genetic diversity taking into account environmental heterogeneity. Mol Ecol Notes 4:139–142
Daly JW, Myers CW (1967) Toxicity in Panamanian poison frogs (Dendrobates): some biological and chemical aspects. Science 156:970–973
Darst CR, Cummings ME, Cannatella DC (2006) A mechanism for diversity in warning signals: conspicuousness versus toxicity in poison frogs. Proc Natl Acad Sci USA 103:5852–5857
Darwin C (1887) The life and letters of Charles Darwin: including an autobiographical chapter, edited by his son Francis Darwin. Murray, London
Donnelly MA (1987) Territoriality in the poison-dart frog *Dendrobates pumilio* (Anura: Dendrobatidae). PhD dissertation, University of Miami
Donnelly MA (1989) Demographic effects of reproductive resource supplementation in a Territorial Frog, *Dendrobates pumilio*. Ecol Monogr 59(3):207–221
Drummond AJ, Rambaut A (2007) BEAST: Bayesian evolutionary analysis by sampling trees. BMC Evol Biol 7:214
Drummond AJ, Rambaut A, Shapiro B, Pybus OG (2005) Bayesian coalescent inference of past population dynamics from molecular sequences. Mol Biol Evol 22:1185–1192
Drummond AJ, Suchard MA, Xie D, Rambaut A (2012) Bayesian phylogenetics with BEAUti and the BEAST 1.7. Mol Biol Evol 29:1969–1973
Dumont BL, Payseur BA (2008) Evolution of the genomic rate of recombination in mammals. Evolution 62:276–294
Edmonds CA, Lillie AS, Cavalli-Sforza LL (2004) Mutations arising in the wave front of an expanding population. Proc Natl Acad Sci USA 101:975–979
Excoffier L, Lischer HEL (2010) Arlequin suite ver 3.5: a new series of programs to perform population genetics analyses under Linux and Windows. Mol Ecol Resour 10:564–567
Excoffier L, Novembre J, Schneider S (2000) SIMCOAL: a general coalescent program for the simulation of molecular data in interconnected populations with arbitrary demography. J Hered 91:506–510
Excoffier L, Foll M, Petit RJ (2009) Genetic consequences of range expansions. Annu Rev Ecol Evol Syst 40:481–501

Fleming K, Johnston P, Zwartz D et al (1998) Refining the eustatic sea-level curve since the Last Glacial Maximum using far- and intermediate-field sites. Earth Planet Sci Lett 163(1–4):327–342
Galbreath KE, Hafner DJ, Zamudio K (2009) When cold is better: climate-driven elevation shifts yield complex patterns of diversification and demography in an alpine specialist (American Pika, *Ochotona princeps*). Evolution 63:2848–2863
GIBCO (2012) GEBCO digital atlas on behalf of the Intergovernmental Oceanographic Commission and the International Hydrographic Organization as part of the general bathymetric chart of the oceans. British Oceanographic Data Centre, Liverpool, UK
Graham CH, van der Wal J, Phillips SJ, Moritz C, Williams SE (2010) Dynamic refugia and species persistence: tracking spatial shifts in habitat through time. Ecography 33:1062–1069
Grant T, Frost DR, Caldwell JP et al (2006) Phylogenetic systematics of dart-poison frogs and their relatives (Amphibia: Athesphatanura: Dendrobatidae). Bull Am Mus Nat Hist 299:1–262
Grant WS, Liu M, Gao T, Yanagimoto T (2012) Limits of Bayesian skyline plot analysis of mtDNA sequences to infer historical demographies in Pacific herring (and other species). Mol Phylogenet Evol 65(1):203–212
Hagemann S, Pröhl H (2007) Mitochondrial paraphyly in a polymorphic poison frog species (Dendrobatidae; *D. pumilio*). Mol Phylogenet Evol 45:740–747
Hauswaldt JS, Ludewig A-K, Vences M, Pröhl H (2010) Widespread co-occurrence of divergent mitochondrial haplotype lineages in a Central American species of poison frog (*Oophaga pumilio*). J Biogeogr 38:711–726
Hegna R, Saporito RA, Donnelly MA (2012) Not all colors are equal: predation and color polytpism in the aposematic poison frog *Oophaga pumilio*. Evol Ecol. doi:10.1007/s10682-012-9605-z
Hewitt GM (1996) Some genetic consequences of iceages, and their role in divergence and speciation. Biol J Linn Soc 58:247–276
Hijmans RJ, Cameron SE, Parra JL, Jones PG, Jarvis A (2005) Very high resolution interpolated climate surfaces for global land areas. Int J Climatol 25:1965–1978
Ho SY, Phillips MJ, Cooper A, Drummond AJ (2005) Time dependency of molecular rate estimates and systematic overestimation of recent divergence times. Mol Biol Evol 22:1561–1568
Ho SY, Lanfear R, Bromham L, Phillips MJ, Soubrier J, Rodrigo AG, Cooper A (2011) Time-dependent rates of molecular evolution. Mol Ecol 20:3087–3101
Klopfstein S, Currat M, Excoffier L (2006) The fate of mutations surfing on the wave of a range expansion. Mol Biol Evol 23:482–490
Lemey P, Rambaut A, Welch JJ, Suchard MA (2010) Phylogeography takes a relaxed random walk in continuous space and time. Mol Biol Evol 27:1877–1885
Limerick S (1980) Courtship behavior and oviposition of the poison-arrow frog *Dendrobates pumilio*. Herpetologica 36(1):69–71
Lohse K, James N, Stone GN (2011) Inferring the colonization of a mountain range-refugia vs. nunatak survival in high alpine ground beetles. Mol Ecol 20:394–408
Maan ME, Cummings ME (2008) Female preferences for aposematic signal components in a polymorphic poison frog. Evolution 62(9):2334–2345
Maan ME, Cummings ME (2009) Sexual dimorphism and directional sexual selection on aposematic signals in a poison frog. Proc Natl Acad Sci USA 106:19072–19077
Maan ME, Cummings ME (2012) Poison frog colors are honest signals of toxicity, particularly for bird predators. Am Nat 179(1):1–14
Maddison DR, Maddison WP (2005) MacClade 4: analysis of phylogeny and character evolution. Version 4.08a. http://macclade.org
Meuche I, Linsenmair KE, Pröhl H (2012) Intrasexual competition, territoriality and acoustic communication in male strawberry poison frogs (*Oophaga pumilio*). Behav Ecol Sociobiol 4:613–621
Milne GA, Long AJ, Bassett SE (2005) Modelling Holocene relative sea-level observations from the Caribbean and South America. Quat Sci Rev 24(10–11):1183–1202
Morgan K, O' Loughlin S, Chen B et al (2011) Comparative phylogeography reveals a shared impact of Pleistocene environmental change in shaping genetic diversity within nine Anopheles mosquito species across the Indo-Burma biodiversity hotspot. Mol Ecol 20:4533–4549
Müller F (1879) Ituna and Thyridia; a remarkable case of mimicry in butterflies (R. Meldola translation). Proc R Entomol Soc 1879:20–29
Phillips SJ, Anderson RP, Schapire RE (2006) Maximum entropy modeling of species geographic distributions. Ecol Model 190:231–259
Piperno DR, Pearsall DM (1998) The origins of agriculture in the lowland Neotropics. Academic Press, San Diego
Posada D (2008) jModelTest: phylogenetic model averaging. Mol Biol Evol 25:1253–1256

Poulton EB (1890) The colours of animals: their meaning and use especially considered in the case of insects. Kegan Paul, Trench, Trubner and Co. Ltd., London
Pröhl H (1997) Territorial behavior of the strawberry poison-dart frog, *Dendrobates pumilio*. Amphib Reptil 18:437–442
Pröhl H, Berke O (2001) Spatial distributions of male and female strawberry poison frogs and their relation to female reproductive resources. Oecol 129:534–542
Pröhl H, Hödl W (1999) Parental investment, potential reproductive rates and mating system in the strawberry poison-dart frog *Dendrobates pumilio*. Behav Ecol Sociobiol 46:215–220
Pröhl H, Ostrowski T (2011) Behavioural elements reflect phenotypic colour divergence in a poison frog. Evol Ecol 25(5):993–1015
Pröhl H, Hagemann S, Karsch J, Hobel G (2007) Geographic variation in male sexual signals in strawberry poison frogs (*Dendrobates pumilio*). Ethology 113(9):825–837
Rambaut A, Drummond AJ (2009) Tracer v1.5. Available at http://beast.bio.ed.ac.uk/Tracer
Ray N, Currat M, Foll M, Excoffier L (2010) SPLATCHE2: a spatially explicit simulation framework for complex demography, genetic admixture and recombination. Bioinformatics 26:2993–2994
Reynolds RG, Fitzpatrick BM (2007) Assortative mating in poison-dart frogs based on an ecologically important trait. Evolution 61:2253–2259
Richards-Zawacki CL, Cummings ME (2011) Intraspecific reproductive character displacement in a polymorphic poison dart frog, *Dendrobates pumilio*. Evolution 65:259–267
Richards-Zawacki CL, Wang IJ, Summers KS (2012) Mate choice and the genetic basis for colour variation in a polymorphic dart frog: inferences from a wild pedigree. Mol Ecol 21:3879–3892
Rudh A, Rogell B, Höglund J (2007) Non-gradual variation in colour morphs of the Strawberry Poison Frog *Dendrobates pumilio*: genetic and geographical isolation suggest a role for selection in maintaining polymorphism. Mol Ecol 16:4284–4294
Rudh A, Rogell B, Håstad O, Qvarnström A (2011) Rapid population divergence linked with co-variation between coloration and sexual display in strawberry poison frogs. Evolution 65(5):1271–1282
Santos JC, Coloma LA, Summers K et al (2009) Amazonian amphibian diversity is primarily derived from late Miocene Andean lineages. PLoS Biol 7:448–461
Saporito R, Donnelly M, Garraffo H et al (2006) Geographic and seasonal variation in alkaloid-based chemical defenses of *Dendrobates pumilio* from Bocas del Toro, Panama. J Chem Ecol 32(4):795–814
Saporito RA, Donnelly MA, Jain P et al (2007) Spatial and temporal patterns of alkaloid variation in the poison frog *Oophaga pumilio* in Costa Rica and Panama over 30 years. Toxicon 50:757–778
Savage JM (2002) The amphibians and reptiles of Costa Rica: a herpetofauna between two continents, between two seas. University of Chicago Press, Chicago
Slatkin M, Maddison WP (1989) A cladistic measure of gene flow inferred from phylogenies of alleles. Genetics 123:603–613
Staudt K, Ospina SM, Mebs D, Pröhl H (2010) Foraging behaviour and territoriality of the strawberry poison frog (*Oophaga pumilio*) in dependence of the presence of ants. Amphib Reptil 31(2):217–227
Summers K, Earn D (1999) The cost of polygyny and the evolution of female care in poison frogs. Biol J Linn Soc 66:515–538
Summers K, Bermingham E, Weight L et al (1997) Phenotypic and genetic divergence in three species of dart-poison frogs with contrasting parental behavior. J Hered 88(1):8–13
Summers K, Symula R, Clough M, Cronin T (1999) Visual mate choice in poison frogs. Proc Roy B Biol Sci 266:2141–2145
Summers K, Cronin TW, Kennedy T (2003) Variation in spectral reflectance among populations of *Dendrobates pumilio*, the strawberry poison frog, in the Bocas del Toro Archipelago, Panama. J Biogeogr 30:35–53
Summers K, Cronin TW, Kennedy T (2004) Cross-breeding of distinct color morphs of the strawberry poison frog (*Dendrobates pumilio*) from the Bocas del Toro Archipelago, Panama. J Herpet 38(1):1–8
Symula R, Schulte R, Summers K (2001) Molecular phylogenetic evidence for a mimetic radiation in Peruvian poison frogs supports a Müllerian mimicry hypothesis. Proc Roy B Biol Sci 268:2405–2421
Tazzyman SJ, Iwasa Y (2010) Sexual selection can increase the effect of random genetic drift—a quantitative genetic model of polymorphism in *Oophaga pumilio*, the strawberry poison dart frog. Evolution 64(6):1719–1728
Voje KL, Hemp C, Flagstad Ø, Saetre GP, Stenseth NC (2009) Climatic change as an engine for speciation in flightless Orthoptera species inhabiting African mountains. Mol Ecol 18:93–108
Wallace AR (1867) Proc Entomol Soc Lond. March 4th: IXXX–IXXXi
Wang IJ (2011) Inversely related aposematic traits: reduced conspicuousness evolves with increased toxicity in a polymorphic poison-dart frog. Evolution 65:1637–1649

Wang IJ, Shaffer HB (2008) Rapid color evolution in an aposematic species: a phylogenetic analysis of color variation in the strikingly polymorphic strawberry poison-dart frog. Evolution 62:2742–2759
Wang IJ, Summers K (2010) Genetic structure is correlated with phenotypic divergence rather than geographic isolation in the highly polymorphic strawberry poison-dart frog. Mol Ecol 19(3):447–458
Weygoldt P (1980) Complex brood care and reproductive behaviour in captive poison-arrow frogs, *Dendrobates pumilio* O. Schmidt. Behav Ecol Sociobiol 7(4):329–332